MT 26 International Conference on Magnet Technology
Vancouver, Canada | 2019

Numerical Analysis of Gradient-Induced Eddy Current in a Superconducting MRI Magnet

Chaoqun Niu, Lei Wang, Yujia Zhai, Yang Liu, Hongyi Qu, Qiuliang Wang

Institute of Electrical Engineering, Chinese Academy of Sciences, Beijing 100190, China
College of Electrical and Information Engineering , Hunan University, Changsha 410082, China

Tue-Mo-Po2.26-06

ABSTRACT

In magnetic resonance imaging (MRI) scanners, eddy currents are inevitably induced by pulsed magnetic gradient fields, which will distort the MRI image and introduce thermal loads in cryostat vessels. For superconducting magnets, heating problem due to induced eddy current is particularly important, which may cause system quench by changing the operating temperature of magnet from desired state. In this paper, eddy currents in a superconducting MRI magnet induced by z-gradient coil and the undesired effects are analyzed. In addition, the eddy current variation and secondary magnetic field B_0-shift caused by mechanical errors are firstly investigated.

INTRODUCTION

Due to the pulsed magnetic gradient field in MRI, eddy currents are inevitably induced in the surrounding conducting components. The eddy current losses in the cryostat become a thermal load of superconducting magnet, which may result in increased boil-off of the cryogens or even magnet quenching in extreme cases. The secondary magnetic field caused by the eddy currents distort the linear gradient fields, leading to the misregistration of MRI signal. A numerical simulation of eddy current effects is vital for their compensation/control and further improvement of MRI technology.

In this paper, a high-efficiency coupled circuit network method is outlined to numerically model the transient eddy current in MRI superconducting magnet. Eddy currents induced by an actively shielded z-gradient coil and their adverse effects are analyzed. Also, effects on eddy currents caused by the misalignment of gradient coil in z direction are also evaluated. It is expected that these results will provide meaningful engineering implication for improving the reliability and stability of superconducting MRI system.

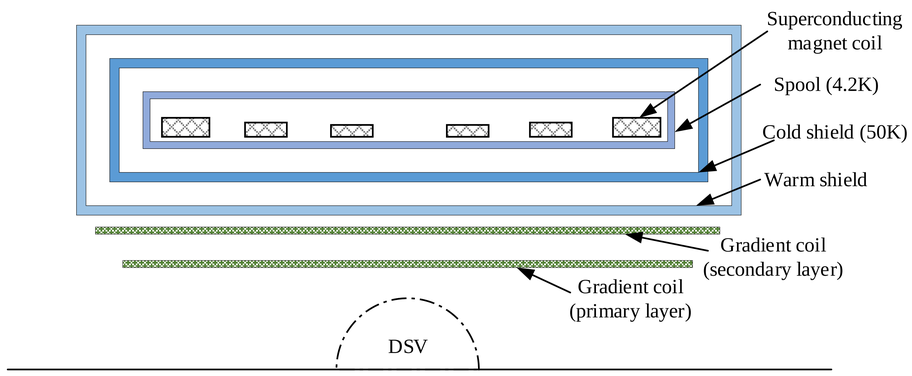

Fig. 1. Axial-symmetric schematic diagram of the model showing the superconducting MRI magnet and actively shielded gradient coil.

METHODOLOGY

Fig. 1 shows a schematic diagram of a gradient coil in a superconducting MRI magnet. The cryostat model consists of three cylindrical conducting structures, including a warm shield, a cold shield and a spool. The gradient coils are located within the warm bore of the magnet with an actively shielded coil to mitigate the induced eddy currents.

As for z-gradient coil, only azimuthal eddy currents are induced in cylindrical conductors. Therefore, the cylindrical structures can be divided into a number of concentric circular slices with a finite thickness to consider the skin depth. The equivalent circuit network model is shown in Fig. 2. According to the basic circuit theory, the simultaneous coupled circuit equations can be written in matrix form as

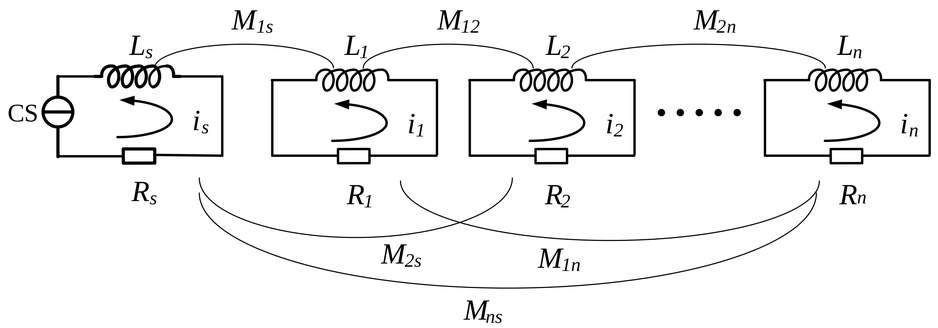

Fig. 2. Equivalent coupled circuit network representation for the coupled gradient coil and circular slices in the conducting structure.

$$\mathbf{M}\frac{d\boldsymbol{i}(t)}{dt}+\mathbf{R}\boldsymbol{i}(t)=-\mathbf{M}_s\frac{di_s(t)}{dt} \tag{1}$$

which **M** and **R** are inductance and resistance matrix, respectively. ***i*** is a vector composed of current in the slices. $\mathbf{M}_s$ is the mutual inductance matrix between gradient coil and slices. i_s is the current in the gradient coil.

The self and mutual inductances of and between the gradient coil and circular slices can be calculated by simple expression in terms of elliptical integration or precise numerical integration. Equation (1) can be simplified into a decoupled differential matrix equation by Eigen matrix technique. Then the time-varying eddy current ***i*** can be solved by the Runge-Kutta method (function *ode-45* in Matlab).

RESULTS AND DISCUSSION

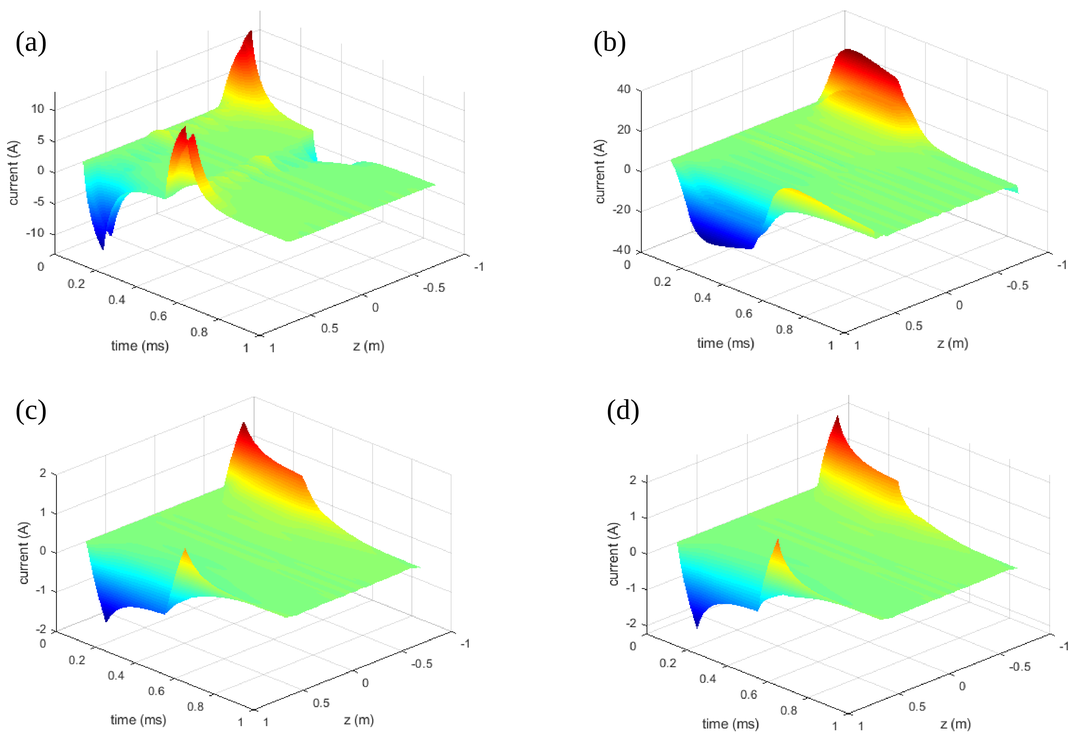

Fig. 3. Eddy currents induced by z-gradient coil in cryostat vessels. (a) Warm shield. (b) Cold shield. (c) First layer of spool. (d) Second layer of spool.

MT 26 International Conference on Magnet Technology
Vancouver, Canada | 2019

Numerical Analysis of Gradient-Induced Eddy Current in a Superconducting MRI Magnet

Chaoqun Niu, Lei Wang, Yujia Zhai, Yang Liu, Hongyi Qu, Qiuliang Wang

Institute of Electrical Engineering, Chinese Academy of Sciences, Beijing 100190, China
College of Electrical and Information Engineering , Hunan University, , Changsha 410082, China

Tue-Mo-Po2.26-06

中国科学院·电工研究所 IEECAS

A. Eddy currents induced by actively shielded z-gradient coil

Fig. 3 shows the transient eddy currents induced in the warm shield, cold shield and spool, respectively. Eddy currents in the warm shield is rapidly dissipated, while eddy currents in the cold shield lasts longer due to the high conductivity of aluminum. In virtue of the high conductivity, the amplitude of the peak eddy current in the cold shield is more than twice as large as that in the warm shield. Otherwise, the peak eddy current in spool is substantially reduced because of the high shielding efficiency of cold shield.

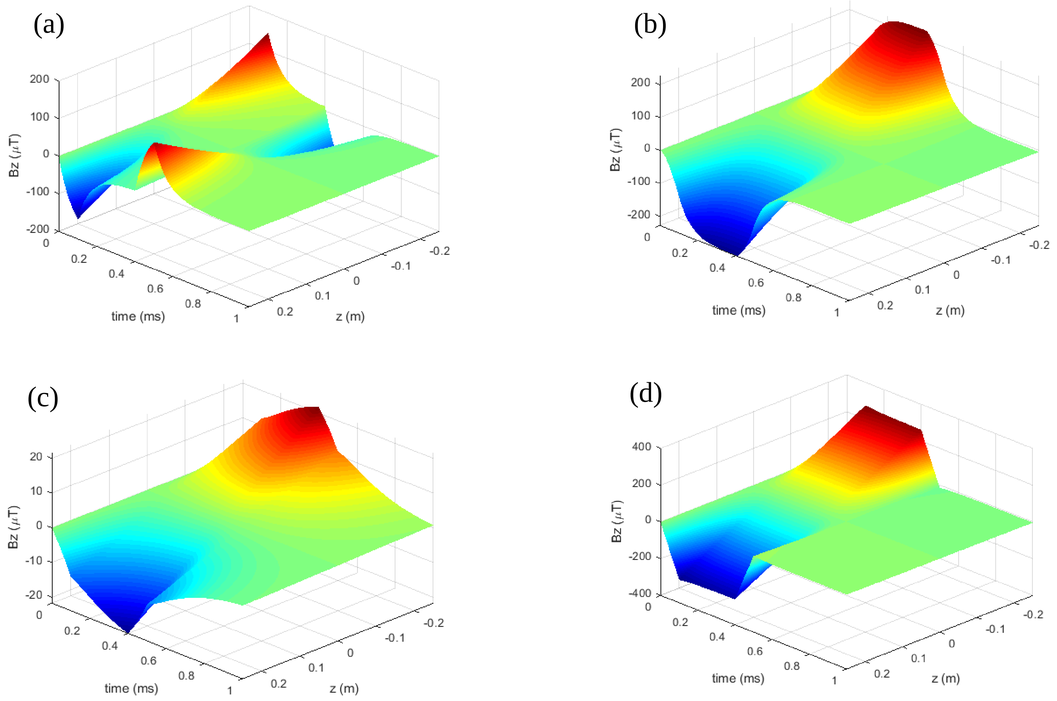

Fig. 4. Transient secondary magnetic field generated by eddy currents. (a) Warm shield. (b) Cold shield. (c) Spool. (d) Total magnetic field.

Fig. 4 shows the transient secondary magnetic fields generated by the eddy currents in all conductors. The temporal characters of secondary magnetic fields in each conductor is the same with that of eddy currents. The peak magnetic field generated by the cold shield is just a little larger than that generated by warm shield because of the larger distance to DSV. As shown in Fig. 4, the secondary magnetic field has a long acting effects on the linear gradient field, which will be aggravated for fast and ultra-fast imaging.

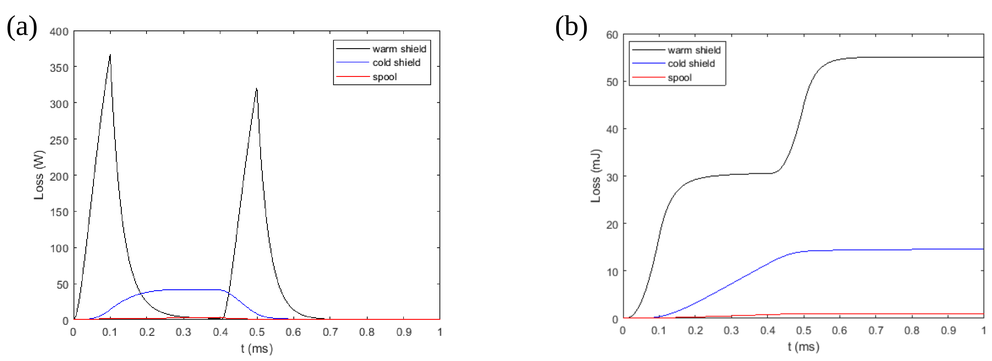

Fig. 5. Power loss generated by eddy current in cryostat vessels. (a)Transient power losses. (b) Accumulated power losses.

Fig. 5 shows the transient and accumulated eddy current losses on the cryostat vessels. Although the eddy current in warm shield is much smaller and dissipates faster than that in cold shield, the power loss in warm shield is much larger because of the high resistivity of stain steel. In addition, the accumulated power loss due to eddy current increase faster with time, which will increase heating load for the superconducting magnet.

B. Eddy current variation caused by mechanical errors

Fig. 6 compares the transient secondary magnetic fields at a point 0.2 m in axial direction in DSV with different misalignment Δ. We can see that the secondary magnetic field increase with Δ, which is caused by the decreased shielding effect of the shielding coil due to mechanical errors.

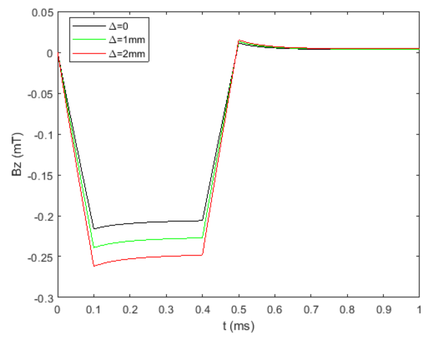

Fig. 6. Comparison of eddy current induced secondary magnetic field with different Δ

Eddy current induced B_0-shift is another adverse effect caused by mechanical errors, which may lead to misregistration of spatial position of the sample. From Fig. 7, we can see that the peak magnitude of B_0-shift increases with Δ. Therefore, it is necessary to minimize the mechanical error during manufacturing and assembling.

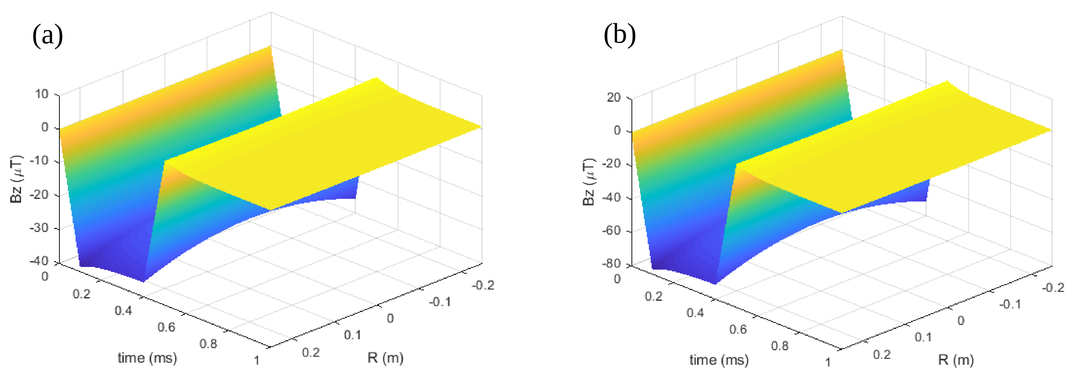

Fig. 7. Eddy current induced B_0-shift caused by different Δ. (a) Δ=1 mm. (b) Δ=2 mm.

CONCLUSION

In this paper, we use coupled circuit network to calculate the eddy current induced in an MRI superconducting magnet by an actively shielded z-gradient coil. The eddy current effects including transient secondary magnetic field and power loss have been analyzed. In addition, the eddy current variation caused by mechanical errors has been investigated. The simulation results show that mechanical error will lead to larger secondary magnetic field in DSV. Also, eddy current induced B_0-shift is introduced, which is harmful to MR imaging.